SUPPORTING INFO

TEMPERATURE-INDUCED STRUCTURE SWITCH IN THERMO-RESPONSIVE MICELLAR INTERPOLYELECTROLYTE COMPLEXES: TOWARD CORE-SHELL-CORONA AND WORM-LIKE MORPHOLOGIES

Claudia Dähling,[a] Gudrun Lotze,[b] Markus Drechsler,[c] Hideharu Mori,[d] Dmitry V. Pergushov,[e] Felix A. Plamper[a]

[a]Institute of Physical Chemistry, RWTH Aachen University, Landoltweg 2, 52056 Aachen, Germany
[b]ESRF - The European Synchrotron, High Brilliance Beamline ID02, 71, Avenue des Martyrs, CS40220, 38043 Grenoble Cedex 9, France
[c]Bayreuth Institute of Macromolecular Chemistry (BIMF), University of Bayreuth, Universitätsstraße 30, 95447 Bayreuth, Germany
[d]Department of Polymer Science and Engineering, Graduate School of Science and Engineering, Yamagata University, 4-3-16 Jonan, Yonezawa 992 8510, Japan
[e]Department of Chemistry, M.V. Lomonosov Moscow State University, Leninskie Gory 1/3, 119991 Moscow, Russia
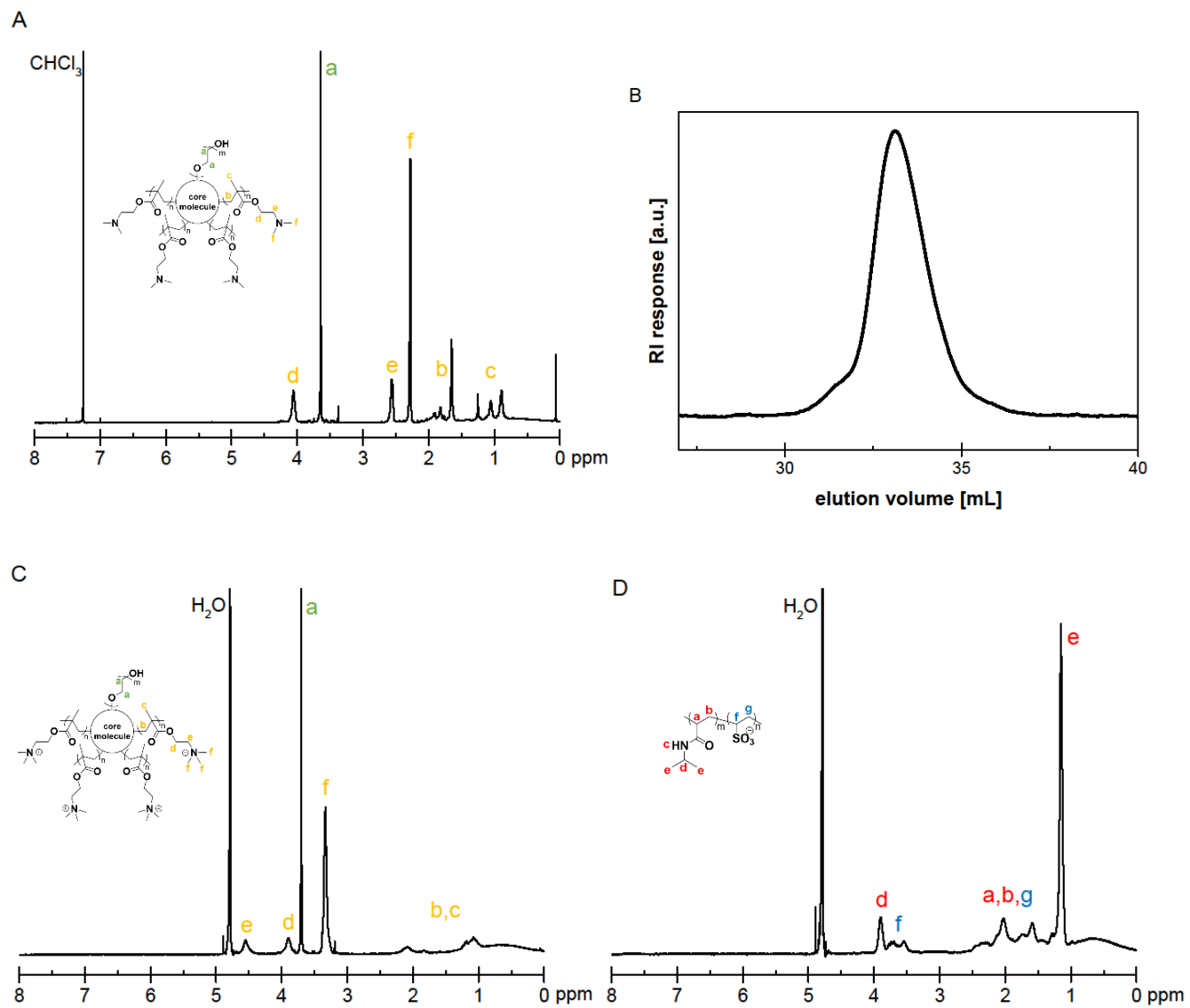
Fig. S1. ^{1}H NMR spectra of (A) PEO$_{114}$-(PDMAEMA$_{17}$)$_4$ in CDCl$_3$, (C) PEO$_{114}$-(qPDMAEMA$_{17}$)$_4$ in D$_2$O, (D) PVS$_{31}$-b-PNIPAM$_{27}$ in D$_2$O and (B) SEC trace of PEO$_{114}$-(PDMAEMA$_{17}$)$_4$ (SEC (DMF 1 g/L LiBr; PEO calibration): M_n = 10500 g/mol, PDI = 1.12).
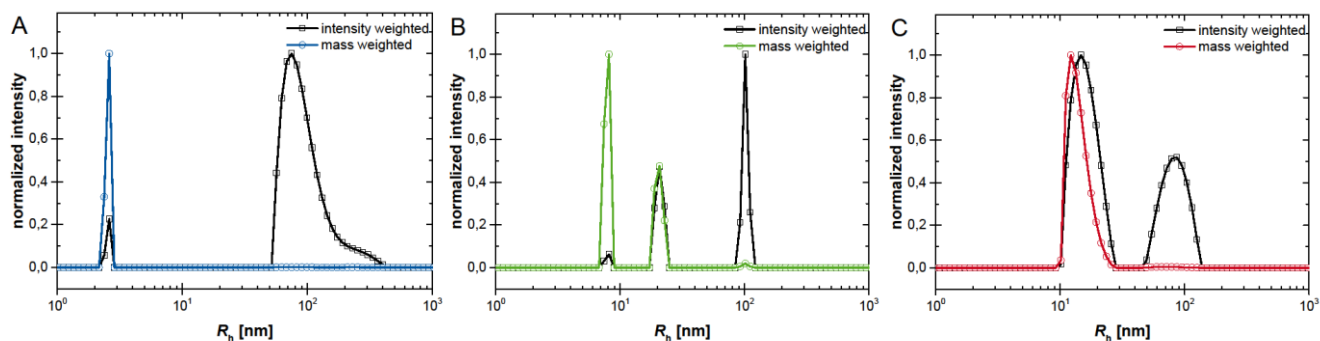
Fig. S2. Intensity- and mass-weighted CONTIN plots of PVS$_{31}$-b-PNIPAM$_{27}$ in dilute (0.4 mg/mL) aqueous solution (0.3 M NaCl) at different temperatures (A: 20 °C, B: 44 °C, C: 60 °C) and a scattering angle of $\Theta = 90°$.

Fig. S3. Intensity- and mass-weighted CONTIN plots of PEO$_{114}$-(qPDMAEMA$_{17}$)$_4$ in dilute (0.8 mg/mL) aqueous solution (0.03 M NaCl) at different temperatures (A: 20 °C, B: 60 °C) and a scattering angle of $\Theta = 90°$.

Fig. S4. Intensity- and mass-weighted CONTIN plots of the IPEC formed by PEO$_{114}$-(qPDMAEMA$_{17}$)$_4$ and PVS$_{31}$-b-PNIPAM$_{27}$ in dilute (1.1 mg/mL) aqueous solution (0.3 M NaCl) at different temperatures (A: 20 °C, B: 44 °C, C: 60 °C) and a scattering angle of $\Theta = 90°$.
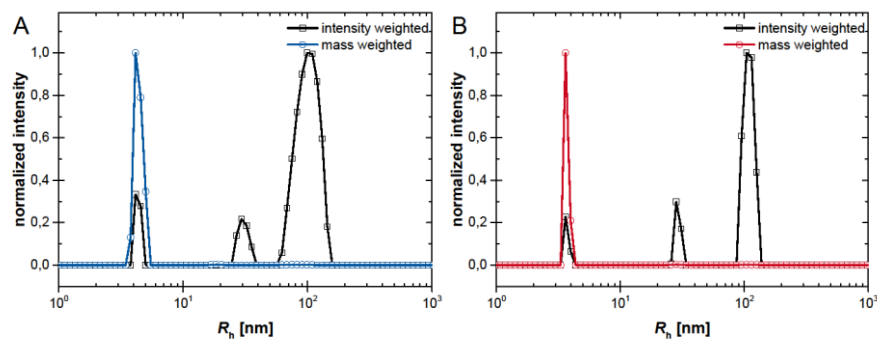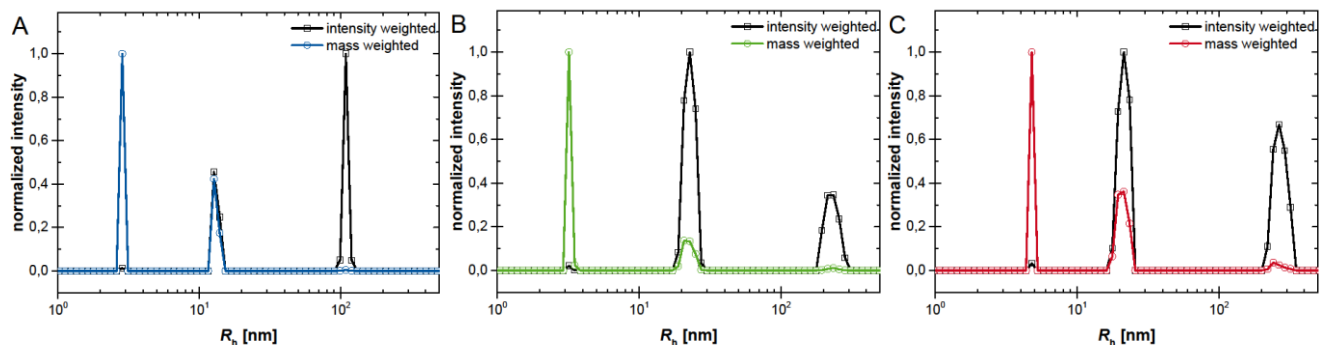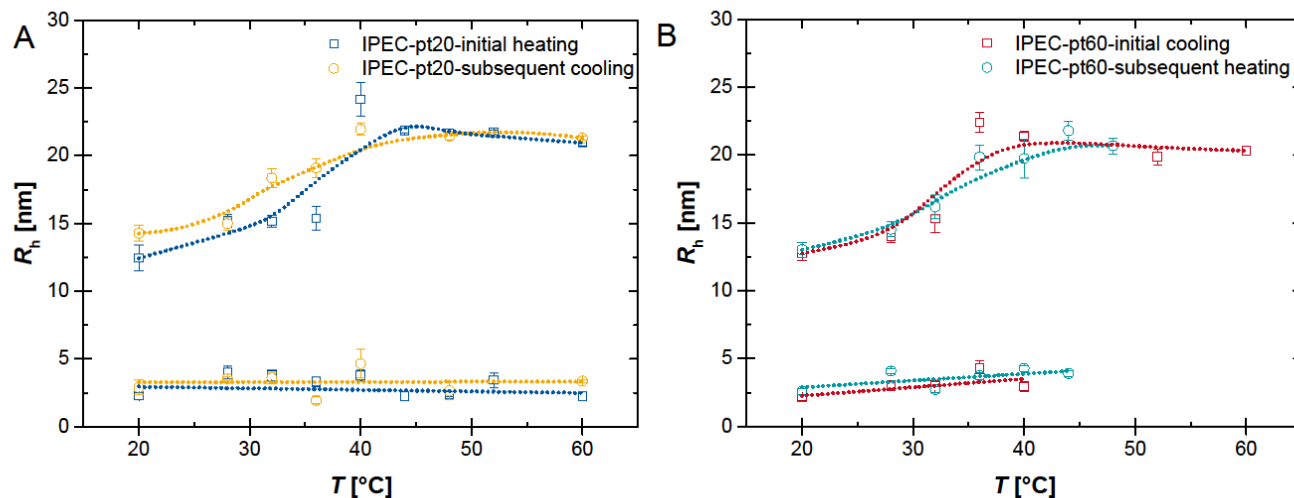
3

Fig. S5. Temperature dependence of the hydrodynamic radius of the IPEC formed by PEO_{114}-$(qPDMAEMA_{17})_4$ and PVS_{31}-b-$PNIPAM_{27}$ in dilute (1.1 mg/mL) aqueous solution (0.3 M NaCl) measured by DLS; A: the IPEC solution was prepared at 22±2 °C heated to 60 °C (IPEC-pt20-initial heating) and cooled to 20 °C (IPEC-pt20-subsequent cooling); B: the IPEC solution was prepared at 60 °C cooled to 20 °C (IPEC-pt60-initial cooling) and heated to 48 °C (IPEC-pt60-subsequent heating). The dotted lines are guides to the eyes.

Table S1: Estimated scattering length densities (SLD) for water and the pure polymer compounds calculated with SASfit software.[1]

	estimated SLD 10^{-5} Å^{-2}
water	0.944
PEO_{114}	1.046
$qPDMAEMA_{68}$	1.237
$PNIPAM_{27}$	1.024
PVS_{31}	1.109

Table S2: Scattering length densities (SLD) obtained from core-shell-shell fits.

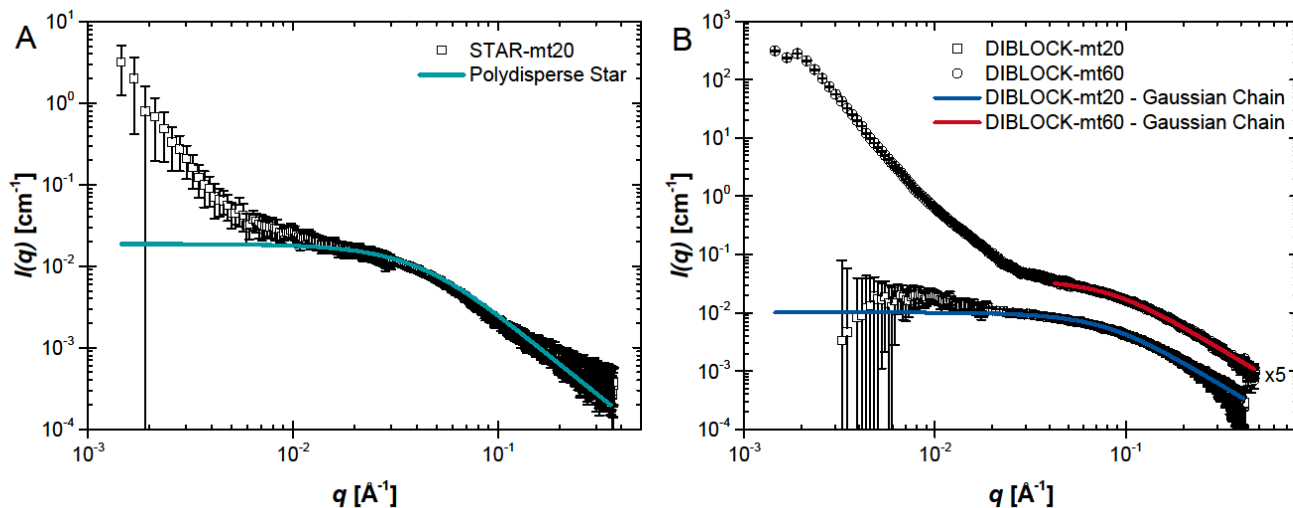| sample	fit	SLD core 10^{-5} Å^{-2}	SLD shell 1 10^{-5} Å^{-2}	SLD shell 2 10^{-5} Å^{-2}
IPEC-20h-pt20-mt20	css	1.515	0.970	0.949
IPEC-10min-pt20-mt20	css	1.313	0.956	0.945
IPEC-20h-pt20-mt60	css	1.030	1.227	0.919
IPEC-20h-pt60-mt60	css	1.030	1.328	0.907
	css +	0.867	1.397	0.934
	cs-cyl	1.083	0.859	
IPEC-10min-pt60-mt60	css	0.948	1.210	0.945

Fig. S6. Scattering curves of samples STAR-mt20 at 20 °C (A) and DIBLOCK-mt20 at 20 °C, DIBLOCK-mt60 at 60 °C (B) in aqueous solution (0.3 M NaCl). The concentration is about 4.6 mg/mL for STAR-mt20 and 2.6 mg/mL for DIBLOCK-mt20 and DIBLOCK-mt60. The solid lines represent fits describing a polydisperse star (A) and a Gaussian chain (B). For clarity, the intensity data for DIBLOCK-mt60 are shifted vertically (x5).

The scattering curve of the diblock copolymer at 20 °C can be described with a model for a Gaussian chain from which we obtain an R_g value of 1.9±0.1 nm (Figure S6, B). Also this value is in accordance to the DLS data. However, at elevated temperatures, the scattering of the micellar diblock copolymer solution turns more complicated, probably due to formation of a small number of pronouncedly scattering loose aggregates. Such a behavior is typical for highly charged polyelectrolytes. Hence, an estimation of the aggregation number of the diblock copolymer micelles is impossible at the conditions used. For q values smaller than 0.04 Å^{-1}, the scattering intensity of the scattering curve recorded at 60 °C rapidly increases indicating the presence of aggregates. For q values above 0.04 Å^{-1}, the scattering curve shows the same shape as that obtained at 20 °C. This can be described with a model for Gaussian polymer chains yielding an R_g of 1.8±0.1 nm. This result might be explained by residual unimeric polymer chains of the diblock copolymer. The reduction in intensity I_0 (forward scattering, as extrapolated to $q = 0$ Å^{-1} from q values above 0.04 Å^{-1}) at 60 °C compared to I_0 obtained below the LCST would indicate that the concentration of unimers is lowered by approximately 25 % upon micellization during heating, presumed that the scattering contrast does not change. As another explanation, it is also possible that the scattering curve describes small length scale substructures of larger particles at these higher q values. According to the DLS measurements, the dominant species at 60 °C are the diblock copolymer micelles with an R_h of about 15 nm which formed at the expense of the diblock copolymer unimers. By DLS, their scattering contribution becomes so weak that their presence could not be clearly indicated at 60 °C. In turn, the presence of micelles could unfortunately not be confirmed within this SAXS study (obscured micellar form factor). There is a rather strong overlap of scattering contributions from the micelles and possible loose aggregates of these highly charged entities. For this, two possible explanations can be considered: First, it is conceivable that most of the micelles have aggregated because sixfold polymer concentrations were used for SAXS measurements compared to the DLS study. Secondly, the scattering contribution of the micellar structures might be hidden because their contribution might be masked by the high scattering intensity of the aggregates.
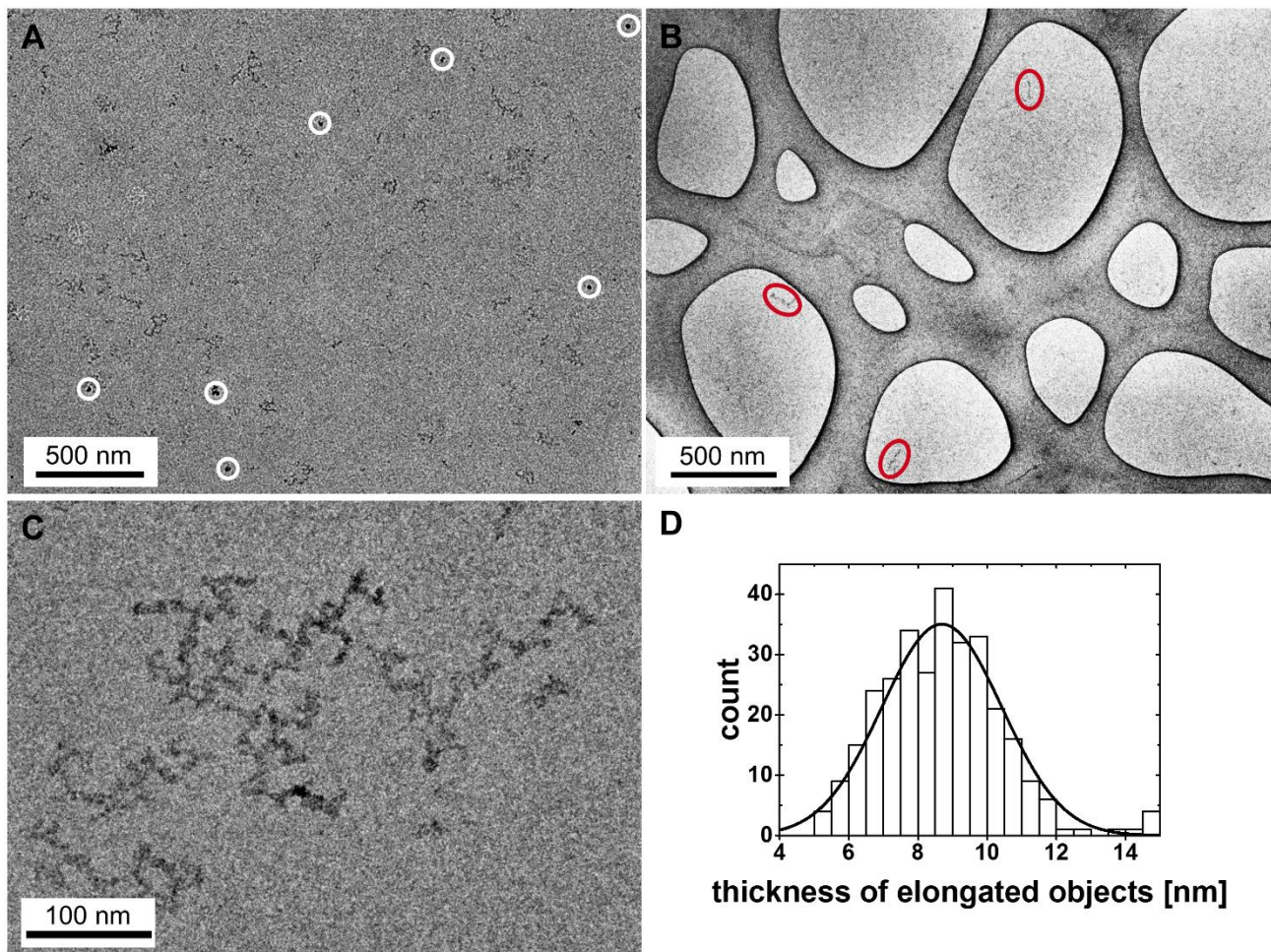
Fig. S7: Cryo-TEM images of an aqueous mixture (0.3 M NaCl) of PEO_{114}-$(qPDMAEMA_{17})_4$ and PVS_{31}-b-$PNIPAM_{27}$ at 60 °C. White circles in A highlight spherical micellar objects with an average radius of 13.9 ± 1.8 nm. Red ellipses in B surround worm-like objects. C shows elongated structures with D giving a histogram of its thickness.
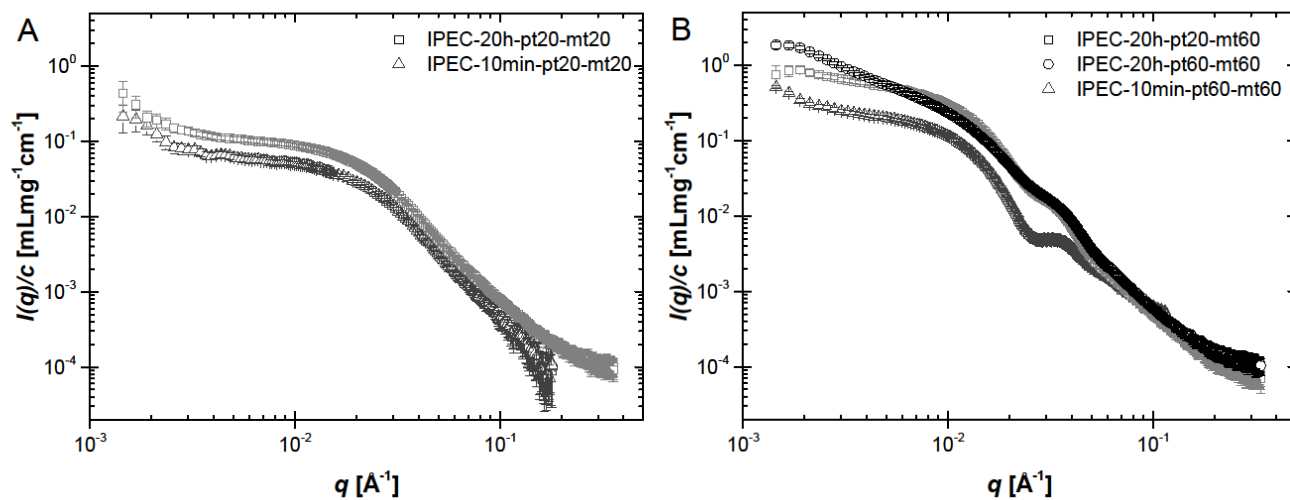

Fig. S8. Scattering curves of IPEC samples in aqueous solution (0.3 M NaCl) at 20 °C (A) and 60 °C (B). The intensity data are normalized to the polymer concentration for better comparison.

The measured SAXS curves were quantitatively analyzed on the basis of the following models:

The scattering data obtained from an aqueous solution of the miktoarm star polymer PEO_{114}-$(qPDMAEMA_{17})_4$ were fitted with a form factor for polydisperse star polymers with Gaussian statistics.[2]

$$I_{\text{PolydisperseStar}}(q) = I_0 \frac{1+\frac{\langle R_g^2 \rangle_z q^2}{3f}}{\left(1+\frac{\langle R_g^2 \rangle_z q^2 (f+1)}{6f}\right)^2}$$

I_0: forward scattering for $q = 0$
f: number of arms
$\langle R_g^2 \rangle_z$: z-average of the squared radius of gyration of an arm

The scattering data obtained from an aqueous solution of the diblock copolymer PVS_{31}-b-$PNIPAM_{27}$ were fitted with a form factor for Gaussian chains.[3]

$$I_{\text{Gauss}}(q) = I_0 2 \frac{exp(-q^2 R_g^2) + q^2 R_g^2 - 1}{(q^2 R_g^2)^2}$$

I_0: forward scattering for $q = 0$
R_g: radius of gyration

The scattering data obtained from an aqueous solution (0.3 M NaCl) of the interpolyelectrolyte complex formed by PEO_{114}-$(qPDMAEMA_{17})_4$ and PVS_{31}-b-$PNIPAM_{27}$ at 20 °C and 60 °C were fitted with a form factor for polydisperse core-shell-shell spheres, based on the below described form factor of a polydisperse core-shell sphere, and polydisperse core-shell cylinders.[4,5]
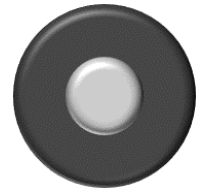
$$P_{\text{core-shell sphere}}(qR_c) = \frac{16\pi^2}{q^6}(\eta_s - \eta_c)^2 \left(c_1 + c_2 qR_c + c_3(qR_c)^2 \left(\frac{Z+2}{Z+1}\right) + B(qR_c)^{(Z+1)/2}\{c_4 \cos[(Z+1)D(qR_c)] + \right.$$
$$c_7 \sin[(Z+1)D(qR_c)]\} + qR_c B(qR_c)^{(Z+2)/2}\{c_5 \cos[(Z+2)D(qR_c)] + c_8 \sin[(Z+2)D(qR_c)]\} +$$
$$\left. \left(\frac{Z+2}{Z+1}\right)(qR_c)^2 B(qR_c)^{(Z+3)/2}\{c_6 \cos[(Z+3)D(qR_c)] + c_9 \sin[(Z+3)D(qR_c)]\}\right)$$

$B(qR_c) = \frac{(Z+1)^2}{(Z+1)^2 + 4(qR_c)^2}$

$D(qR_c) = \tan^{-1}\left(\frac{2qR_c}{Z+1}\right)$

$c_1 = \frac{1}{2} - \gamma(\cos[qD_s] + qD_s \sin[qD_s]) + \frac{\gamma}{2}(1 + (qD_s)^2)$

$c_2 = \gamma qD_s(\gamma - \cos[qD_s])$

$c_3 = \frac{\gamma^2 + 1}{2} - \gamma \cos[qD_s]$

$c_4 = \gamma^2(qD_s \cos[qD_s] - \sin[qD_s])^2 - c_1$

$c_5 = 2\gamma \sin[qD_s][1 - \gamma(qD_s \sin[qD_s] + \cos[qD_s])] + c_2$

$c_6 = c_3 - \gamma^2 \sin^2[qD_s]$

$c_7 = \gamma \sin[qD_s] - \frac{\gamma^2}{2}(1 + (qD_s)^2)\sin[2qD_s] - c_5$

$c_8 = c_4 - \frac{1}{2} + \gamma \cos[qD_s] - \frac{\gamma^2}{2}(1 + (qD_s)^2)\cos[2qD_s]$

$c_9 = \gamma \sin[qD_s](1 - \gamma \cos[qD_s])$

D_s: shell thickness
R_c: average radius of the core
η_s, η_c, η_m: scattering length density of the shell, the core, the suspension medium

Z: related to polydispersity σ_c of the particle core radius R_c by $\sigma_c^2 = \left(\frac{\overline{R_c^2}}{\overline{R_c}^2} - 1\right) = \frac{1}{Z+1}$ and originates from Schulz distribution $G(R_c) =$

$\frac{R_c^Z}{\Gamma(Z+1)}\left(\frac{Z+1}{\overline{R_c}}\right)^{Z+1} \exp\left[-\frac{R_c}{\overline{R_c}}(Z+1)\right]$
γ: scaled medium contrast, $\gamma = \frac{\eta_m - \eta_s}{\eta_c - \eta_s}$

$$I_{\text{core-shell cylinder}}(q) = \text{bkg} + \frac{scale}{\pi R_c^2 L_c}\sum_{R_c} n(R_c, \sigma_c)P(q, R_c, R_{cs}, L_c, L_{cs}, \rho_c, \rho_{cs}, \rho_{solv})$$

$$n(R_c) = \frac{exp\left(-\frac{1}{2}\left[\frac{\ln(R_c/R_0)}{\sigma_c}\right]^2\right)}{\sqrt{2\pi}\sigma_c R_c}$$

$$P_{\text{core-shell cylinder}}(q) = \int_0^{\pi/2} \sin\theta \cdot d\theta \cdot \left[\pi R_{cs}^2 L_{cs}(\rho_{cs} - \rho_{solv})\frac{\sin\left(\frac{qL_{cs}\cos\theta}{2}\right)}{\frac{qL_{cs}\cos\theta}{2}}\frac{2J_1(qR_{cs}\sin\theta)}{qR_{cs}\sin\theta} + \pi R_c^2 L_c(\rho_c - \rho_{cs})\frac{\sin\left(\frac{qL_c\cos\theta}{2}\right)}{\frac{qL_c\cos\theta}{2}}\frac{2J_1(qR_c\sin\theta)}{qR_c\sin\theta}\right]^2$$

J_1: first order Bessel function
θ: angle between cylinder axis and scattering vector q
R_c: core radius

L_c: core length

R_0: mean core radius

$R_{cs} = R_c + D_s$: entire radius with radial shell thickness D_s
$L_{cs} = L_c + 2 \cdot face\ thickness$: entire length

σ_c: standard deviation of the log-normal distribution $n(R_c)$

REFERENCES

1. I. Breßler, J. Kohlbrecher and A. F. Thünemann, *J. Appl. Crystallogr.*, 2015, **48**, 1587-1598.
2. W. Burchard, *Macromolecules*, 1974, **7**, 835-841.
3. P. Debye, *J. Phys. Colloid Chem.*, 1947, **51**, 18-32.
4. P. Bartlett and R. H. Ottewill, *J. Chem. Phys.*, 1992, **96**, 3306-3318.
5. S. A. Rice, *J. Polym. Sci.*, 1956, **19**, 594-594.